CrystEngComm

RSC Publishing

PAPER

View Article Online
View Journal | View Issue



Cite this: *CrystEngComm*, 2013, **15**, 10068

# Do perfluoroarene···arene and C–H···F interactions make a difference to the structures of 4,2':6',4''-terpyridine-based coordination polymers?†

Edwin C. Constable,*[a] Catherine E. Housecroft,*[a] Srboljub Vujovic,[a] Jennifer A. Zampese,[a] Aurélien Crochet[b] and Stuart R. Batten[c]

The consequences for the structures of coordination polymers of introducing fluoro substituents into the terminal phenyl domain of 4'-(biphenyl-4-yl)-4,2':6',4''-terpyridine (**1**) have been investigated. Reaction between $Cu(OAc)_2{\cdot}H_2O$ and 4'-(2',3',4',5',6'-pentafluorobiphenyl-4-yl)-4,2':6',4''-terpyridine (**2**) yields the one-dimensional coordination polymer $[Cu_2(\mu\text{-}OAc)_4(\mathbf{2})]_n$ which contains paddle-wheel $\{Cu_2(OAc)_4\}$ nodes bridged by ligands **2**. The compound is isostructural with $[Cu_2(\mu\text{-}OAc)_4(\mathbf{1})]_n$. When $Cu(OAc)_2{\cdot}H_2O$ reacts with a 1 : 1 mixture of **1** and **2**, $[Cu_2(\mu\text{-}OAc)_4(\mathbf{1})]_n$ and $[Cu_2(\mu\text{-}OAc)_4(\mathbf{2})]_n$ co-crystallize with **1** and **2** disordered over one ligand site; the one-dimensional coordination polymer is isostructural with each of $[Cu_2(\mu\text{-}OAc)_4(\mathbf{1})]_n$ and $[Cu_2(\mu\text{-}OAc)_4(\mathbf{2})]_n$ indicating that replacing H by F substituents in the peripheral arene ring has no effect on the overall solid-state structure: tpy···tpy π-stacking is preserved, arene···arene $\pi_H\cdots\pi_H$ interactions are replaced by perfluoroarene···arene $\pi_F\cdots\pi_H$ interactions, and H···H contacts are replaced by H···F interactions. In stark contrast to the latter observations, the reaction of $Zn(OAc)_2{\cdot}2H_2O$ with perfluoro derivative **2** yields $[Zn_5(OAc)_{10}(\mathbf{2})_4{\cdot}11H_2O]_n$ as the dominant one-dimensional polymer; minor amounts of the anticipated polymer $[Zn_2(\mu\text{-}OAc)_4(\mathbf{2})]_n$ are also formed. The solid-state structure of $[Zn_5(OAc)_{10}(\mathbf{2})_4{\cdot}11H_2O]_n$ consists of quadruple-stranded polymer chains assembled from $\{Zn_5(\mathbf{2})_4\}$ subchains interconnected by $\{Zn_5(OAc)_{10}\}$ units. Within each chain, $\pi_F\cdots\pi_F$ and $\pi_H\cdots\pi_H$ stacking interactions are dominant, while the observed assembly of chains into sheets and π-stacking between arene units in adjacent sheets mimic the dominant interactions in the single-stranded chains observed in $[Zn_2(\mu\text{-}OAc)_4(\mathbf{1})]_n$, $[Zn_2(\mu\text{-}OAc)_4(\mathbf{2})]_n$, $[Cu_2(\mu\text{-}OAc)_4(\mathbf{1})]_n$, $[Cu_2(\mu\text{-}OAc)_4(\mathbf{2})]_n$ and $[Cu_2(\mu\text{-}OAc)_4(\mathbf{1})]_n{\cdot}[Cu_2(\mu\text{-}OAc)_4(\mathbf{2})]_n$.

Received 15th July 2013,
Accepted 19th September 2013

DOI: 10.1039/c3ce41384e

www.rsc.org/crystengcomm

## Introduction

The replacement of hydrogen in a compound by fluorine not only influences the physical and chemical properties of the compound[1], but may also significantly alter solid-state packing interactions. The classic example concerns the crystal packing in solid benzene or hexafluorobenzene *versus* a 1 : 1 co-crystallized mixture. Both $C_6H_6$[2] and $C_6F_6$[3] exhibit edge-to-face CX···π interactions (X = H[4–6] or F[7]), while the co-crystallized material has infinite columns of alternating $C_6D_6$ and $C_6F_6$ molecules which interact through π-stacking interactions.[8,9] Molecular assembly directed by such arene···perfluoroarene interactions is now well recognized.[10,11] A wider perspective has been taken by Hulliger and coworkers who have surveyed the roles played in crystal engineering by phenyl···perfluorophenyl (abbreviated as $\pi_H\cdots\pi_F$), CF···H, F···F and CF···$\pi_F$ interactions; they concluded (in 2005) that 'the role of fluorine in crystal engineering is not yet clear in detail'.[12] An update of this picture appeared in 2011, adding CF···$M^+$, CF···C=O and anion···$\pi_F$ contacts to packing interactions in fluorine-containing compounds.[13] A study of the packing of partially fluorinated diphenylethynes underlines the importance of phenyl···perfluorophenyl stacking but questions the stabilizing effects of CH···F and CF···F contacts.[14] Although $\pi_H\cdots\pi_F$ stacking has gained significant attention in crystal engineering and has been utilized to direct host–guest complex formation,[15] the coexistence of arene and perfluoroarene rings does not necessarily result in such interactions. Competitive packing motifs may predominate, and hydrogen bonds in particular are favoured over $\pi_H\cdots\pi_F$ contacts.[13] (The strength of the face-to-face $\pi_H\cdots\pi_F$ interaction is *ca.* 20 to 25 kJ

[a] *Department of Chemistry, University of Basel, Spitalstrasse 51, CH-4056 Basel, Switzerland. E-mail: catherine.housecroft@unibas.ch; Fax: +41 61 267 1018; Tel: +41 61 267 1008*
[b] *Department of Physics, University of Fribourg, Chemin du Musée 3, CH-1700 Fribourg, Switzerland. E-mail: aurelien.crochet@unifr.ch*
[c] *School of Chemistry, Monash University, Victoria 3800, Australia. E-mail: stuart.batten@monash.edu*

† Electronic supplementary information (ESI) available: Fig. S1–S3. Powder diffraction patterns for bulk samples. CCDC 949632–949635. For ESI and crystallographic data in CIF or other electronic format see DOI: 10.1039/c3ce41384e

mol$^{-1}$.[11]) More subtle factors may also tip the balance. For example, the compounds shown in Scheme 1a crystallize with no face-to-face $\pi_H\cdots\pi_F$ interactions.[16] In contrast, the molecules of a related 2,2'-bipyridine derivative with X = F (Scheme 1b) pack with $\pi_H(py)\cdots\pi_F$ interactions, while co-crystallization of the two compounds in Scheme 1b leads to a crystal lattice containing efficient $\pi_H\cdots\pi_F$ contacts.[17]

Surprisingly, the use of phenyl···perfluorophenyl interactions to direct the assembly of coordination polymers has received little attention. Two examples with related ligands present contrasting packing motifs, with the presence of an ethyne unit in the first example apparently playing a critical role. Reaction of 1,4-bis(4'-pyridylethynyl)tetrafluorobenzene (Scheme 1a, top) with zinc(II) nitrate results in the formation of a one-dimensional polymer in which zig-zag chains interact with each other through $\pi_{alkyne}\cdots\pi_F$ and $\pi_{alkyne}\cdots\pi_{pyridine}$ interactions; there is no $\pi_H\cdots\pi_F$ stacking.[16] The related ligand 1,4-bis(4'-pyridylmethyl)tetrafluorobenzene reacts with $Cd(NO_3)_2$ and aniline to give a one-dimensional coordination polymer in which $\{Cd(NO_3)_2(C_6H_5NH_2)_2\}$ nodes are connected by bridging ligands. In this case, adjacent chains interact through $\pi_H\cdots\pi_F$ stacking. However, replacing aniline by 4-bromoaniline turns off the inter-chain $\pi_H\cdots\pi_F$ interactions.[18]

We have recently reported the assembly of coordination polymers containing the functionalized 4,2':6',4''-terpyridine **1** (Scheme 2) and have discussed the role that face-to-face π-stacking of pairs of biphenyl domains and pairs of tpy units plays in the organization of polymers formed in reactions of **1** with $Zn(OAc)_2{\cdot}2H_2O$, $Cu(OAc)_2{\cdot}H_2O$ and $Cd(OAc)_2{\cdot}2H_2O$.[19] We now report the preparation of compound **2** and investigate the structural consequences of introducing the perfluorophenyl domain. The coordination behaviour of **2** with $Cu(OAc)_2$ and $Zn(OAc)_2$ is described, along with the effect of treating $Cu(OAc)_2$ with a 1:1 mixture of ligands **1** and **2**.

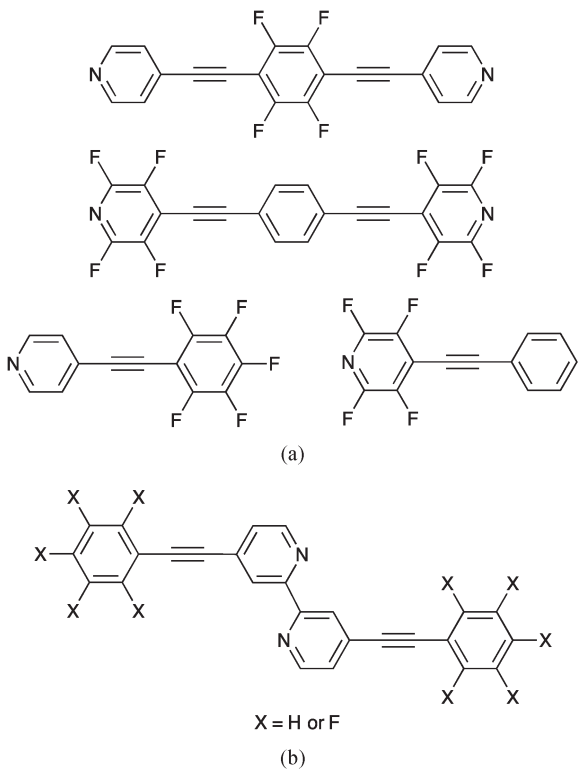


**Scheme 1** (a) Examples of compounds that crystallize with no $\pi_H\cdots\pi_F$ stacking interactions and (b) related compounds which when co-crystallized exhibit $\pi_H\cdots\pi_F$ contacts.

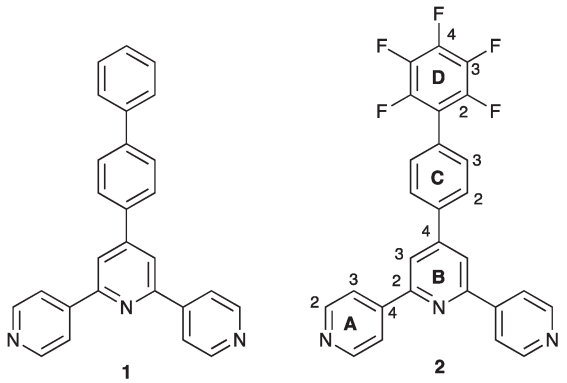


**Scheme 2** Ligand structures and numbering for NMR spectroscopic assignments.

## Experimental

### General

$^1$H, $^{13}$C and $^{19}$F NMR spectra were recorded on a Bruker DRX-500 NMR spectrometer. $^1$H and $^{13}$C NMR chemical shifts were referenced to residual solvent peaks with respect to $\delta$(TMS) = 0 ppm; for $^{19}$F, an external reference of $CFCl_3$ ($\delta$ = 0 ppm) was used. FT-IR spectra were recorded using a Shimadzu FTIR 8400S spectrophotometer with solid samples introduced in a Golden Gate ATR. Electrospray ionisation (ESI) mass spectra were measured on a Bruker Esquire 3000 plus. Solution electronic absorption spectra were recorded on an Agilent 8453 spectrophotometer.

2',3',4',5',6'-Pentafluorobiphenyl-4-carbaldehyde was prepared according to the literature.[20]

### Compound 2

4-Acetylpyridine (1.7 g, 13.7 mmol) was added to a solution of 2',3',4',5',6'-pentafluorobiphenyl-4-carbaldehyde (1.87 g, 6.87 mmol) in EtOH (25 cm$^3$). KOH pellets (0.77 g, 13.7 mmol) were added in one portion, followed by aqueous $NH_3$ (25%, 25 cm$^3$). The reaction mixture was stirred at room temperature for 20 h, during which time a white precipitate formed. This solid was collected by filtration, washed well with $H_2O$ and EtOH, and dried *in vacuo* over $P_2O_5$. Compound **2** was recrystallized from EtOH and was isolated as a white solid (0.733 g, 22.5%). Decomp. > 290 °C. $^1$H NMR (500 MHz, $CDCl_3$) $\delta$/ppm: 8.82 (d, $J$ = 6.1 Hz, 4H, $H^{A2}$), 8.10 (d, $J$ = 6.2 Hz, 4H, $H^{A3}$), 8.09 (s, 2H, $H^{B3}$), 7.89 (d, $J$ = 8.5 Hz, 2H, $H^{C2}$), 7.5 (d, $J$ = 8.6 Hz, 2H, $H^{C3}$). $^{13}$C NMR (126 MHz, $CDCl_3$) $\delta$/ppm: 155.6 ($C^{B2}$), 150.7 ($C^{A2}$), 150.4 ($C^{B4}$), 146.0 ($C^{A4}$), 139.1 ($C^{C1}$), 131.3 ($C^{C3}$), 127.7 ($C^{C2+C4}$), 121.3 ($C^{A3}$),

119.1 ($C^{B3}$), 114.9 ($C^{D1}$), signals for $C^{D2,D3,D4}$ not resolved. $^{19}$F NMR (376 MHz, $CDCl_3$) $\delta$/ppm: −143.0 (m, 2F, $F^{D2/D3}$), −154.3 (m, 1F, $F^{D4}$), −161.5 (m, 2F, $F^{D2/D3}$). IR (solid, $\nu$/cm$^{-1}$): 3035 (w), 1705 (w), 1595 (s), 1513 (m), 1480 (s), 1393 (m), 1318 (w), 1276 (w), 1217 (w), 1194 (w), 1132 (w), 1090 (w), 1061 (m), 1042 (w), 985 (s), 897 (w), 859 (m), 852 (m), 827 (s), 814 (m), 780 (m), 749 (w), 737 (m), 718 (w), 680 (s), 621 (s). UV-vis (EtOH, 2.5 × 10$^{-4}$ mol dm$^{-3}$) $\lambda$/nm: 225 ($\varepsilon$/dm$^3$ mol$^{-1}$ cm$^{-1}$: 26 500), 268 (43 100). ESI MS (MeCN) $m/z$ 476.1 $[M + H]^+$ (calc. 476.1). Found: C 67.52, H 3.26, N 8.55; $C_{27}H_{14}F_5N_3$ requires C 68.21, H 2.97, N 8.84%.

### $[Cu_2(\mu\text{-}OAc)_4(2)]_n$

A solution of **2** (23.6 mg, 0.050 mmol) in $CHCl_3$ (6.0 mL) was placed in a long test tube. MeOH (3.0 mL) was layered on the top of the solution, and then a solution of $Cu(OAc)_2{\cdot}H_2O$ (18.5 mg, 0.1 mmol) in MeOH (5.0 mL) was added carefully over the pure MeOH layer. The tube was sealed with parafilm and left to stand for 3 weeks at room temperature. The turquoise-green crystals of $[Cu_2(OAc)_4(2)]_n$ that had formed were isolated by decantation. Yield: 25.2 mg, 0.030 mmol, 60%. Found: C 50.21, H 3.54, N 5.05; $C_{35}H_{26}Cu_2F_5N_3O_8$ requires C 50.12, H 3.12, N 5.01%.

### $[Cu_2(\mu\text{-}OAc)_4(1)]_n{\cdot}[Cu_2(\mu\text{-}OAc)_4(2)]_n$

A solution of **1** (9.64 mg, 0.025 mmol) and **2** (11.9 mg, 0.025 mmol) in $CHCl_3$ (6.0 mL) was placed in a long test tube. MeOH (3.0 mL) was layered on the top of the first solution, followed by a solution of $Cu(OAc)_2{\cdot}H_2O$ (18.5 mg, 0.1 mmol) in MeOH (5.0 mL). The test tube was sealed with parafilm and allowed to stand for 1 week at room temperature, after which time turquoise-green crystals had formed. Yield: 15.5 mg, 0.0098 mmol, 39.1%. Single crystals of $\{[Cu_2(OAc)_4(1)]_n\}{\cdot}\{[Cu_2(OAc)_4(2)]_n\}$ were separated by decantation. Found: C 52.46, H 3.75, N 5.62; $C_{70}H_{57}Cu_4F_5N_6O_{16}$ requires C 52.96, H 3.62, N 5.29%.

### Reaction of $Zn(OAc)_2{\cdot}2H_2O$ with 2

A solution of **2** (23.6 mg, 0.050 mmol) in $CHCl_3$ (6.0 mL) was placed in a long test tube, and MeOH (3.0 mL) was then layered on top. A solution of $Zn(OAc)_2{\cdot}2H_2O$ (21.8 mg, 0.1 mmol) in MeOH (5.0 mL) was then added carefully, and the tube was sealed with parafilm. After 10 days at room temperature, colourless crystals had formed. These proved to be a mixture of colourless blocks of $[Zn_2(OAc)_4(2)]_n$ and colourless plates of $[Zn_5(OAc)_{10}(2)_4{\cdot}11H_2O]_n$. See text for bulk sample analysis.

### $[Cd_2(\mu\text{-}OAc)_4(2)_2]_n$

A solution of **2** (23.6 mg, 0.050 mmol) in $CHCl_3$ (6.0 mL) was placed in a long test tube, and MeOH (3.0 mL) was layered on top of the solution. A solution of $Cd(OAc)_2{\cdot}2H_2O$ (26.7 mg, 0.100 mmol) in MeOH (5.0 mL) was added carefully, and the tube was sealed with parafilm and left for 3 weeks at room temperature. Over this period, colourless crystals formed and were isolated by decantation. Satisfactory analysis on the bulk sample could not be obtained.

## Crystallography

Single crystal data were collected on a Bruker APEX-II diffractometer with data reduction, solution and refinement using the programs APEX[21] and SHELXL-97 or SHELX-13.[22] The ORTEP-type diagram and structure analysis used Mercury v. 3.0.[23,24] Powder diffractograms were measured on a STOE STADI P diffractometer equipped with Cu K$\alpha$1 radiation ($\lambda$ = 1.540598 Å) and a Mythen1K detector.

### Compound 2

$C_{27}H_{14}F_5N_3$, $M$ = 475.41, colourless block, monoclinic space group $Cc$, $a$ = 10.6918(11), $b$ = 17.4451(17), $c$ = 10.9674(11) Å, $\beta$ = 96.054(4)°, $U$ = 2034.2(4) Å$^3$, $Z$ = 4, $D_c$ = 1.552 Mg m$^{-3}$, $\mu$(Cu-K$\alpha$) = 1.071 mm$^{-1}$, $T$ = 123 K. Total 15 280 reflections, 3453 unique, $R_{int}$ = 0.0281. Refinement of 3414 reflections (316 parameters) with $I > 2\sigma(I)$ converged at final $R_1$ = 0.0293 ($R_1$ all data = 0.0296), w$R_2$ = 0.0777 (w$R_2$ all data = 0.0782), gof = 1.061. CCDC 949634.

### $[Cu_2(OAc)_4(2)]_n$

$C_{35}H_{26}Cu_2F_5N_3O_8$, $M$ = 838.69, green block, monoclinic space group $C2/c$, $a$ = 26.5522(13), $b$ = 16.7313(9), $c$ = 8.0639(4) Å, $\beta$ = 107.038(3)°, $U$ = 3425.2(3) Å$^3$, $Z$ = 4, $D_c$ = 1.626 Mg m$^{-3}$, $\mu$(Cu-K$\alpha$) = 2.282 mm$^{-1}$, $T$ = 123 K. Total 18 388 reflections, 3059 unique, $R_{int}$ = 0.0417. Refinement of 2718 reflections (322 parameters) with $I > 2\sigma(I)$ converged at final $R_1$ = 0.0610 ($R_1$ all data = 0.0672), w$R_2$ = 0.1639 (w$R_2$ all data = 0.1696), gof = 1.114. CCDC 949632.

### $[Cu_2(OAc)_4(1)]_n{\cdot}[Cu_2(OAc)_4(2)]_n$

$C_{70}H_{57}Cu_4F_5N_6O_{16}$, $M$ = 1587.42, green block, monoclinic space group $C2/c$, $a$ = 26.366(3), $b$ = 16.393(2), $c$ = 8.1433(9) Å, $\beta$ = 107.648(6)°, $U$ = 3354.2(7) Å$^3$, $Z$ = 2, $D_c$ = 1.572 Mg m$^{-3}$, $\mu$(Cu-K$\alpha$) = 2.182 mm$^{-1}$, $T$ = 123 K. Total 14 871 reflections, 2950 unique, $R_{int}$ = 0.0306. Refinement of 2663 reflections (245 parameters) with $I > 2\sigma(I)$ converged at final $R_1$ = 0.0502 ($R_1$ all data = 0.0541), w$R_2$ = 0.1518 (w$R_2$ all data = 0.1560), gof = 1.125. CCDC 949633.

### $[Zn_5(OAc)_{10}(2)_4{\cdot}11H_2O]_n$

$C_{128}H_{108}F_{20}N_{12}O_{31}Zn_5$, $M$ = 3017.26, colourless plate, monoclinic space group $Cc$, $a$ = 39.181(2), $b$ = 16.5180(9), $c$ = 25.5638(14) Å, $\beta$ = 129.465(3)°, $U$ = 12772.9(13) Å$^3$, $Z$ = 4, $D_c$ = 1.557 Mg m$^{-3}$, $\mu$(Cu-K$\alpha$) = 2.019 mm$^{-1}$, $T$ = 123 K. Total 18 388 reflections, 20 471 unique, $R_{int}$ = 0.0445. Refinement of 15 051 reflections (1879 parameters) with $I > 2\sigma(I)$ converged at final $R_1$ = 0.0683 ($R_1$ all data = 0.0962), w$R_2$ = 0.1802 (w$R_2$ all data = 0.2057), gof = 1023. CCDC 949635.

 

## Results and discussion

### Synthesis and characterization of compound 2

Compound **2** is conveniently prepared using the one pot method of Hanan[25] by reacting 2',3',4',5',6'-pentafluorobiphenyl-4-carbaldehyde with two equivalents of 4-acetylpyridine in basic EtOH in the presence of $NH_3$ (Scheme 3). The base peak (*m*/*z* 476.1) in the electrospray mass spectrum of **2** was assigned to $[M + H]^+$, and the $^1H$, $^{13}C$ and $^{19}F$ NMR spectra were in accord with the structure of **2** shown in Scheme 3. $^1H$ and $^{13}C$ NMR spectra were assigned using COSY, HMQC and HMBC techniques. The resonance for the *ipso*-carbon of the fluorinated ring ($C^{D1}$) was located using an HMBC cross peak between $H^{C3}$ and $C^{D1}$; multiplets for the remaining $^{13}C$ signals in ring D were not resolved. Fig. 1 compares the absorption spectra of compounds **1** and **2**; the introduction of the fluoro substituents blue-shifts the most intense absorption from 278 to 268 nm.

Single crystals of **2** were grown from a $CHCl_3$ solution layered with hexane. The compound crystallizes in the monoclinic space group *Cc*, and the structure is shown in Fig. 2; bond lengths and angles are unexceptional. The tpy domain is close to planar, and the pentafluorophenyl ring also lies approximately in this plane, with the phenylene ring showing a significant twist. Using the ring labelling in Scheme 2, the angles between ring planes are A/B = 9.6 and 6.3°, B/C = 34.9° and C/D = 32.5°; twisting of B/C and C/D pairs of rings minimizes repulsions between *ortho* substituents on adjacent rings, whether they be H or F atoms. In contrast to **2**, compound **1** crystallizes in the space group $P2_1/c$ with five independent molecules which possess significant differences in conformation.[19] Crystal packing in **1** involves π-stacking and CH···N interactions. However, the conformational variation among independent molecules precludes a simple packing description. In contrast, slipped $\pi_H(py)\cdots\pi_F$ contacts between molecules of **2** result in the assembly of chains which run parallel to the *c*-axis (Fig. 3a). However, the π interaction is not optimal; the pentafluorophenyl ring lies between two pyridine rings with $\pi_F$ centroid$\cdots\pi_H$(py) centroid

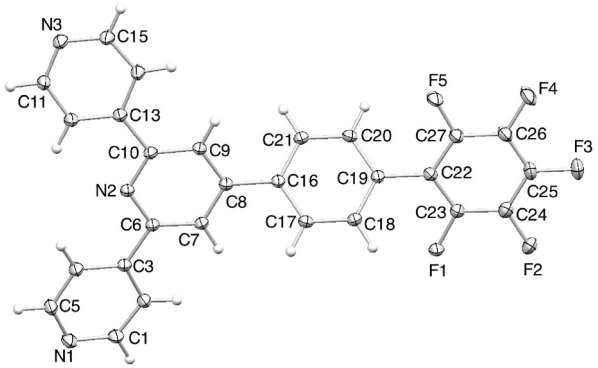


**Fig. 2** ORTEP diagram of the structure of **2** (ellipsoids were plotted at the 40% probability level).

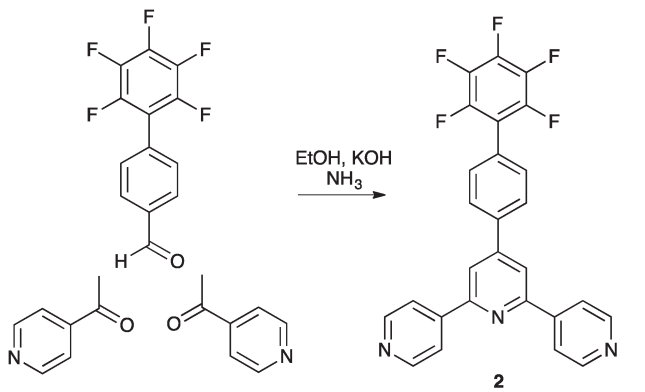


**Scheme 3** Synthetic route to compound **2**.

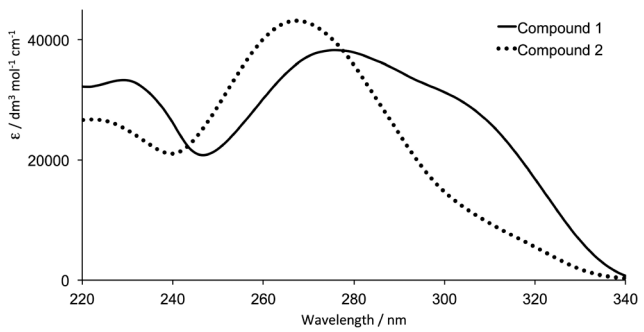


**Fig. 1** Absorption spectra of EtOH solutions of compounds **1** and **2**.

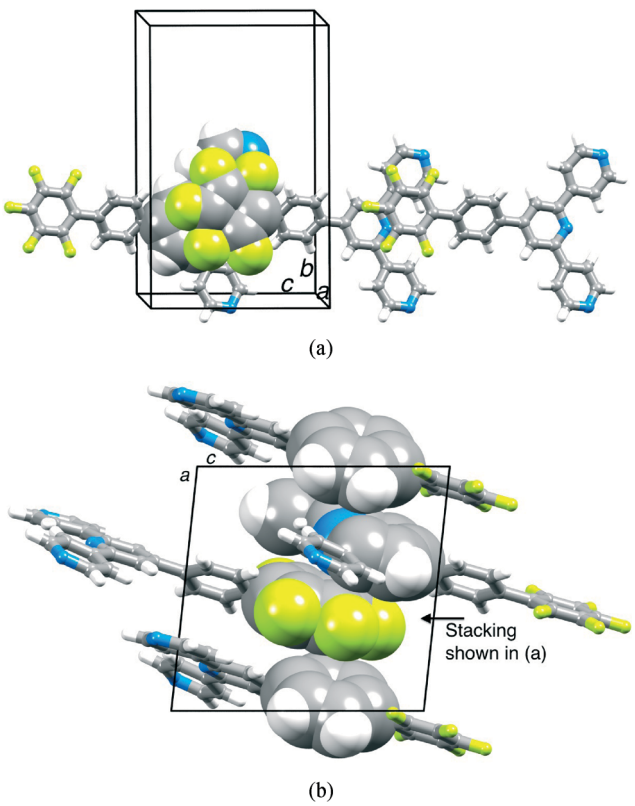


**Fig. 3** Packing interactions in **2**: (a) chains following the *c*-axis with slipped intermolecular $\pi_H(py)\cdots\pi_F$ contacts and (b) relatively inefficient π-stacking (space-filling representation) along the *a*-axis. H and F atoms are shown in white and green, respectively.

distances of 4.24 and 3.88 Å. Packing of adjacent chains involves weak $\pi_H$(py)···$\pi_H$(arene) and $\pi_H$(arene)···$\pi_F$ contacts (Fig. 3b), but the interplane angles and centroid···centroid separations (14.6° with 4.21 Å and 16.3° with 4.63 Å) are outside the limits for efficient interactions. Additional CH···N and CH···F contacts contribute to the overall packing between the chains. We note that the structure of 4'-pentafluoro-2,2':6',2''-terpyridine has been reported, but the packing has not been discussed.[26] Inspection of the structure (CSD[27] refcode NAZYOE) shows that the pentafluorophenyl unit is sandwiched between two tpy domains of adjacent molecules, with a stacking interaction with respect to each tpy similar to that in **2**.

In the context of the coordination polymers discussed later in this work, it is significant that the solid-state structures of **1** and **2** differ. We investigated the co-crystallization of **1** and **2** from $CH_2Cl_2$/MeOH layered with hexane, but X-ray diffraction analysis of single crystals from these mixtures revealed the growth of separate crystals of **1**[19] and **2**, with structures identical to those previously determined.

### The coordination polymer $[Cu_2(\mu\text{-OAc})_4(2)]_n$

Ligand **1** reacts with copper(II) acetate or zinc(II) acetate to give isostructural coordination polymers in which paddle-wheel $\{M_2(\mu\text{-OAc})_4\}$ units are connected through bridging ligands **1** to form infinite zig-zag chains. Adjacent chains associate through a combination of face-to-face stacking of pairs of biphenyl domains and pairs of tpy domains.[19] Slow diffusion of a chloroform solution of **2** into a methanol solution of $Cu(OAc)_2{\cdot}H_2O$ resulted in the growth of X-ray quality crystals of $[Cu_2(\mu\text{-OAc})_4(2)]_n$. Elemental analysis of the bulk sample was in accord with this formulation, and the powder diffraction pattern for the bulk sample was in agreement with that calculated from the single crystal data (Fig. S1†). Like $[Cu_2(\mu\text{-OAc})_4(1)]_n$,[19] $[Cu_2(\mu\text{-OAc})_4(2)]_n$ crystallizes in the monoclinic space group $C2/c$, and the cell dimensions for the two structures are very similar: for $[Cu_2(\mu\text{-OAc})_4(2)]_n$, $a$ = 26.5522(13), $b$ = 16.7313(9), $c$ = 8.0639(4) Å, $\beta$ = 107.038(3)°, $U$ = 3425.2(3) Å$^3$ compared to parameters for $[Cu_2(\mu\text{-OAc})_4(1)]_n$ of $a$ = 26.0528(9), $b$ = 16.1512(9), $c$ = 8.2267(3) Å, $\beta$ = 108.113(2)°, $U$ = 3290.1(2) Å$^3$. Structural analysis of $[Cu_2(\mu\text{-OAc})_4(2)]_n$ confirmed that the compound is essentially isostructural with $[Cu_2(\mu\text{-OAc})_4(1)]_n$ and revealed that replacement of the pendant phenyl ring in **1** by a pentafluorophenyl unit in **2** has little effect on the structure at either the local or long-range level. Paddle-wheel $\{Cu_2(OAc)_4\}$ units are connected by bridging ligands **2**, with the central N atom of **2** (N2) remaining uncoordinated. The acetato ligands are disordered, and each has been modelled over two positions with site occupancies of 0.36/0.64 and 0.40/0.60, respectively. The asymmetric unit contains half of ligand **2** and half of one $\{Cu_2(\mu\text{-OAc})_4\}$ unit, and the second half of the repeat unit of the polymer is generated by a 2-fold axis (Fig. 4). The Cu–Cu distance of 2.6358(8) Å is typical of the 1046 structures containing $\{Cu_2(\mu\text{-OAc})_4\}$ cores in the Cambridge Structural Database, CSD[27] (Conquest v. 1.15, CSD v. 5.34 with November 2013 updates).[23]

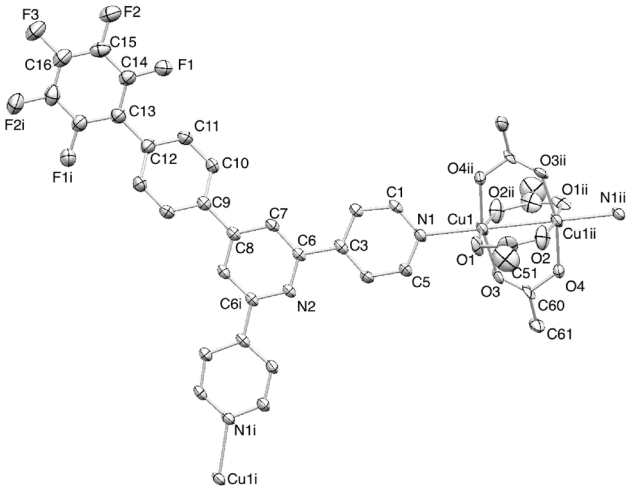


**Fig. 4** ORTEP representation of the repeat unit in $[Cu_2(\mu\text{-OAc})_4(2)]_n$ (ellipsoids were plotted at the 30% probability level, and H atoms were omitted for clarity). Only one occupancy site of each disordered acetato ligand is shown. Symmetry codes: i = 1 − $x$, $y$, 3/2 − $z$; ii = 1/2 − $x$, 7/2 − $y$, 2 − $z$. Selected bond lengths: Cu1–O1 = 1.799(6), Cu1–O3 = 1.955(6), Cu1–O2$^{ii}$ = 2.030(7), Cu1–O4$^{ii}$ = 2.039(6), Cu1–N1 = 2.186(2), Cu1–Cu1$^{ii}$ = 2.6358(8) Å.

Packing of zig-zag chains in $[Cu_2(\mu\text{-OAc})_4(2)]_n$ involves the organization of chains into sheets and π-stacking interactions between arene domains in adjacent sheets. The left-hand part of Fig. 5a illustrates how the pentafluorophenyl unit slots into the V-shaped cavity of a tpy domain of the next chain

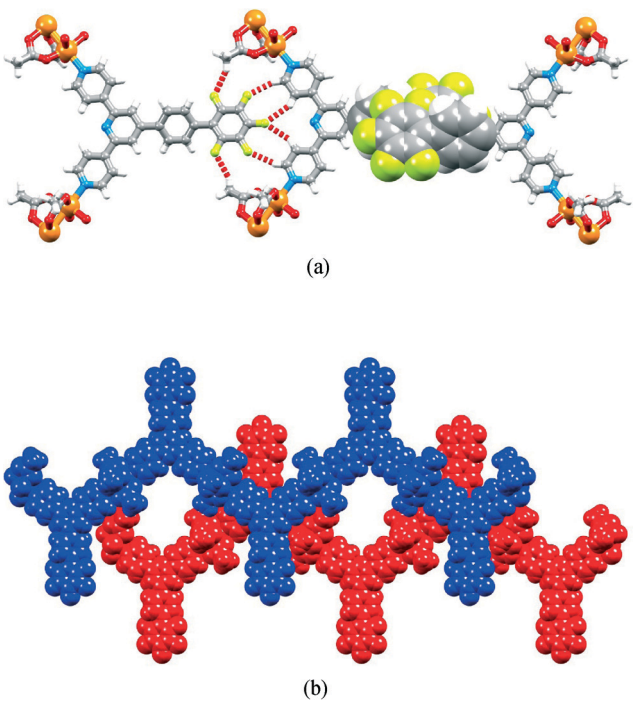


**Fig. 5** Packing motifs in $[Cu_2(\mu\text{-OAc})_4(2)]_n$: (a) short CH···F contacts shown in red (left) and $\pi_H{\cdots}\pi_F$ interactions shown in space-filling representation (right); (b) tpy···tpy π interactions between zig-zag chains.

with short $CH_{methyl}\cdots F$ (2.51 Å) and $CH_{tpy}\cdots F$ contacts (2.42 and 2.54 Å). Although attractive in nature, these interactions are apparently not significant in terms of assisting assembly of the chains into sheets since CH···F interactions in $[Cu_2(\mu\text{-}OAc)_4(2)]_n$ are replaced by CH···H contacts in $[Cu_2(\mu\text{-}OAc)_4(1)]_n$.[19] Chains in adjacent sheets in $[Cu_2(\mu\text{-}OAc)_4(2)]_n$ exhibit the same tpy···tpy π interactions (Fig. 5b) that are observed in a number of related structures containing functionalized 4,2':6',4''-terpyridines and $\{Zn_2(\mu\text{-}OAc)_4\}$ or $\{Cu_2(\mu\text{-}OAc)_4\}$ nodes.[19,28–30] Pyridine rings with N1 and N2 engage in face-to-face contacts with those containing $N1^{iii}$ and $N2^{iii}$ (symmetry code iii = $1-x$, $3-y$, $2-z$) at a separation of 3.48 Å. These are complemented by head-to-tail stacking of pentafluorobiphenyl domains giving $\pi_H\cdots\pi_F$ interactions (Fig. 5a, right-hand side). However, the twist angle of 31.5° between the bonded $C_6F_5$ and $C_6H_4$ rings reduces the efficiency of the interaction, with the angle between the stacked rings necessarily also being 31.5°.

### Co-crystallization of $[Cu_2(\mu\text{-}OAc)_4(1)]_n$ and $[Cu_2(\mu\text{-}OAc)_4(2)]_n$

To further investigate the effects (or lack thereof) of replacing a phenyl by pentafluorophenyl substituent on crystal packing, we reacted $Cu(OAc)_2{\cdot}H_2O$ with a 1 : 1 mixture of ligands **1** and **2**. Elemental analysis of the bulk sample was consistent with an overall stoichiometry of $[Cu_2(\mu\text{-}OAc)_4(1)]_n{\cdot}[Cu_2(\mu\text{-}OAc)_4(2)]_n$. The product crystallized in the monoclinic *C*2/*c* space group with cell dimensions essentially the same as those of $[Cu_2(\mu\text{-}OAc)_4(1)]_n$ and $[Cu_2(\mu\text{-}OAc)_4(2)]_n$. Structural analysis confirmed not only the formation of $[Cu_2(\mu\text{-}OAc)_4(1)]_n{\cdot}[Cu_2(\mu\text{-}OAc)_4(2)]_n$ but also the fact that the asymmetric unit contains the two ligands superimposed; the terminal phenyl/pentafluorophenyl ring is disordered and has been modelled with a 0.5/0.5 site occupancy of each of ligands **1** and **2**. An ordered structure with alternating ligands **1** and **2** along the polymer chain would require a bigger unit cell resulting in more observable reflections, but no additional reflections were observed between the original intensities. This confirms that the only meaningful way to describe the structure is with a disordered model. The metrical parameters of the $\{Cu_2(\mu\text{-}OAc)_4\}$ unit in $[Cu_2(\mu\text{-}OAc)_4(1)]_n{\cdot}[Cu_2(\mu\text{-}OAc)_4(2)]$ (Cu1–O1 = 1.9740(16), Cu1–O3 = 1.974(2), Cu1–$O2^{ii}$ = 1.9599(19), Cu1–$O4^{ii}$ = 1.962(2), Cu1–N1 = 2.1763(19), Cu1–$Cu1^{ii}$ = 2.6326(7) Å, symmetry code as in Fig. 4) are comparable with those in $[Cu_2(\mu\text{-}OAc)_4(1)]_n$. The disorder in $[Cu_2(\mu\text{-}OAc)_4(2)]_n$ (see above) makes comparison less meaningful.

The powder diffraction pattern for the bulk sample was in accord with the pattern calculated from the single crystal diffraction data (Fig. S2†).

### Reaction of $Zn(OAc)_2{\cdot}2H_2O$ with **2**

Knowing that $Zn(OAc)_2{\cdot}2H_2O$ reacts with **1** and a number of other 4'-functionalized 4,2':6',4''-terpyridines[19,28–30] to give one-dimensional polymers with the same assembly motifs as $[Cu_2(\mu\text{-}OAc)_4(1)]_n$ and $[Cu_2(\mu\text{-}OAc)_4(2)]_n$, we expected that reaction of $Zn(OAc)_2{\cdot}2H_2O$ with **2** would give $[Zn_2(\mu\text{-}OAc)_4(1)]_n$. We have observed that the structural paradigm may be modified if the 4'-substituent is 4-(dodecyloxy)phenyl,[31] or 4-(anthracen-9-yl)phenyl,[32] and with 4'-(4-(naphthalen-1-yl)phenyl)-4,2':6',4''-terpyridine (**3**), crystals of both $[Zn_2(\mu\text{-}OAc)_4(3)]_n$ and $[Zn_7(\mu\text{-}OAc)_{10}(\mu_4\text{-}O)_2(3)]_n$ have been isolated from the same crystal growth experiment.[32]

Reaction of **2** with two equivalents of $Zn(OAc)_2{\cdot}2H_2O$ yielded colourless blocks and plates in the same crystallization tube. Preliminary crystal data for the colourless blocks confirmed this to be the one-dimensional coordination polymer $[Zn_2(\mu\text{-}OAc)_4(2)]_n$ which crystallizes in the monoclinic space group *C*2/*c* and possesses the same gross structure as $[Zn_2(\mu\text{-}OAc)_4(1)]_n$,[19] $[Cu_2(\mu\text{-}OAc)_4(1)]_n$[19] and $[Cu_2(\mu\text{-}OAc)_4(2)]_n$. Repeated attempts to obtain a good quality crystal were unsuccessful. X-Ray analysis of the colourless plates revealed the formation of $[Zn_5(OAc)_{10}(2)_4{\cdot}11H_2O]_n$ with an unexpected one-dimensional polymer assembly in which four bridging ligands **2** are associated with five zinc atoms. The repeat unit (Fig. 6) contains five crystallographically independent zinc atoms; Zn1 and Zn5 are tetrahedrally sited, while Zn2, Zn3 and Zn4 are 6-coordinate (Table 1). The coordination environments of Zn1 and Zn5 are similar, each zinc(II) being bound by two monodentate (terminal) acetato ligands, one N donor of a bridging ligand **2** and one O donor of a bridging acetato ligand. The monodentate acetato ligands containing O1/O2 and O17/O18 are disordered, and each has been modelled over two sites of occupancies 0.51/0.49 and 0.54/0.46, respectively. The $N_2O_4$-coordination shell of each of Zn2, Zn3 and Zn4 contains *trans*-N donors, and the acetato ligands that connect them adopt either a μ-O,O' or μ,$\kappa^3$-O,O':O' mode. The Zn···Zn separations along the $\{Zn_5(OAc)_{10}\}$ chain are listed in Table 1; we note the appreciably longer separations associated with the $\{Zn_2(\mu\text{-}O,O'\text{-}OAc)\}$ *versus* $\{Zn_2(\mu\text{-}O,O'\text{-}OAc)(\mu,\kappa^3\text{-}O,O':O'\text{-}OAc)\}$ units. A search of the CSD[27] (Conquest v. 1.15, CSD v. 5.34 with November 2012 updates)[23] did not reveal any pentametal (M = any metal) building blocks that are structurally analogous to the

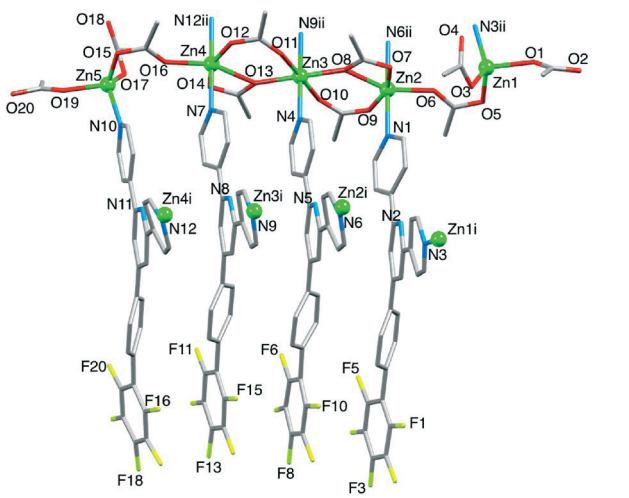


**Fig. 6** Repeat unit of the polymer $[Zn_5(OAc)_{10}(\mathbf{2})_4{\cdot}11H_2O]_n$. Symmetry codes: i = *x*, −*y*, 1/2 + *z*; ii = *x*, −*y*, −1/2 + *z*.

**Table 1** Selected bond distances for $[Zn_5(OAc)_{10}(\mathbf{2})_4{\cdot}11H_2O]_n$. See Fig. 6 caption for symmetry codes

| Bond | Bond distance/Å | Bond | Bond distance/Å |
|---|---|---|---|
| Zn1–O1 | 2.062(4) | Zn5–O15 | 1.981(2) |
| Zn1–O3 | 2.007(3) | Zn5–O17 | 1.996(4) |
| Zn1–O5 | 2.008(2) | Zn5–O19 | 1.9538(19) |
| Zn1–N3$^{ii}$ | 2.079(3) | Zn5–N10 | 2.048(3) |
| Zn2–O6 | 2.0450(13) | Zn3–O8 | 2.1288(17) |
| Zn2–O7 | 2.123(2) | Zn3–O10 | 2.1133(19) |
| Zn2–O8 | 2.2560(14) | Zn3–O11 | 2.0939(19) |
| Zn2–O9 | 1.990(2) | Zn3–O13 | 2.1280(17) |
| Zn2–N6$^{ii}$ | 2.224(3) | Zn3–N9$^{ii}$ | 2.100(3) |
| Zn2–N1 | 2.232(3) | Zn3–N4 | 2.122(3) |
| Zn4–O12 | 2.019(2) | Zn4–O13 | 2.2889(14) |
| Zn4–O16 | 2.0305(14) | Zn4–N7 | 2.181(2) |
| Zn4–O14 | 2.128(2) | Zn4–N12$^{ii}$ | 2.202(3) |
| Zn1···Zn2 | 4.4346(8) | Zn2···Zn3 | 3.8241(8) |
| Zn4···Zn5 | 4.6079(8) | Zn3···Zn4 | 3.8844 (8) |

$\{Zn_5(OAc)_{10}\}$ unit in $[Zn_5(OAc)_{10}(\mathbf{2})_4{\cdot}11H_2O]_n$, although several examples of coordination polymers and networks containing $\{Zn_3(\mu\text{-O,O'-}O_2CR)_2(\mu,\kappa^3\text{-O,O':O'-}O_2CR)_2\}$,[33–37] or $\{Zn_3(\mu\text{-O,O'-}O_2CR)_4(\mu,\kappa^3\text{-O,O':O'-}O_2CR)_2\}$,[38–44] units have been reported.

Each ligand **2** coordinates only through the outer pyridine rings, as is typical for 4,2':6',4''-terpyridines. Fig. 6 illustrates that Zn2, Zn3 and Zn4 are connected to two ligands **2**, while each of Zn1 and Zn5 is bonded to only one. The connectivities are such that $\{Zn_5(\mathbf{2})_4\}$ units (black arrow in Fig. 7a) are interconnected by $\{Zn_5(OAc)_{10}\}$ units (red arrow in Fig. 7a) to generate infinite polymer chains that run parallel to the *c*-axis (Fig. 7a and b). Fig. 7b illustrates how the domains of four pentafluorobiphenyl units protrude from either side of the chain. The four ligands **2** present in the repeat unit shown in Fig. 6 engage in face-to-face stacking of tpy domains and of pentafluorobiphenyl domains, and the efficiencies of the interactions can be assessed from the parameters given in Table 2.

When viewed through the π-stacked domains, the chains exhibit a similar zig-zag appearance to the single chains in $[Zn_2(\mu\text{-OAc})_4(\mathbf{1})]_n$,[19] $[Zn_2(\mu\text{-OAc})_4(\mathbf{2})]_n$, $[Cu_2(\mu\text{-OAc})_4(\mathbf{1})]_n$[19] and $[Cu_2(\mu\text{-OAc})_4(\mathbf{2})]_n$. As in $[Cu_2(\mu\text{-OAc})_4(\mathbf{2})]_n$ (described above), this involves assembly of chains into sheets and π-stacking between arene units in adjacent sheets. Fig. 8 illustrates the packing of two adjacent chains within one sheet (blue and green chains) and between two chains in adjacent sheets (red and blue chains). The latter is comparable to that shown in Fig. 5b. We cannot comment on the role played by the water molecules in $[Zn_5(OAc)_{10}(\mathbf{2})_4{\cdot}11H_2O]_n$. Hydrogen atoms on the water solvates could not be located reliably from the difference map and were not included in the model.

In order to gain insight into the composition of the bulk crystalline material, all crystals (except for those used for single crystal X-ray diffraction) were collected and ground to a powder. The powder pattern for the bulk material is shown in Fig. S2.† When matched to patterns simulated from single crystal data for $[Zn_5(OAc)_{10}(\mathbf{2})_4{\cdot}11H_2O]_n$ and $[Zn_2(\mu\text{-OAc})_4(\mathbf{2})]_n$, the data reveal that $[Zn_5(OAc)_{10}(\mathbf{2})_4{\cdot}11H_2O]_n$ is the dominant component. The sample contains residual $Zn(OAc)_2{\cdot}H_2O$ but no free ligand **2**. The powder pattern also indicates the presence of an additional unknown component.

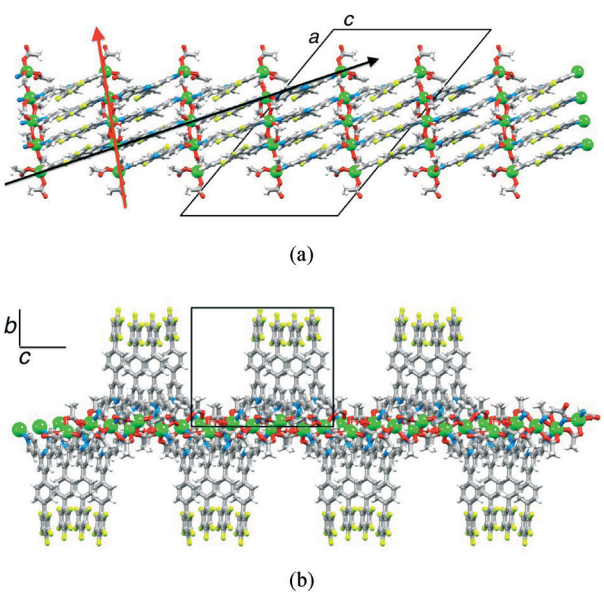


**Fig. 7** Assembly of deep chains in $[Zn_5(OAc)_{10}(\mathbf{2})_4{\cdot}11H_2O]_n$. (a) The red and black arrows define the directionalities of the $\{Zn_5(OAc)_{10}\}$ and $\{Zn_5(\mathbf{2})_4\}$ units, respectively. (b) Chains run along the *c*-axis, and groups of four adjacent pentafluorobiphenyl domains engage in $\pi_F\cdots\pi_F$ and $\pi_H\cdots\pi_H$ stacking interactions.

### Comments on the variation in metal assembly motifs

Dimetallic $\{M_2(\mu\text{-}O_2CR)_4\}$ paddle-wheel building blocks (Scheme 4a) are frequently used to direct the assemblies of coordination polymers and metal–organic frameworks (MOFs).[45–47] Kühn and coworkers have emphasized that the final assembly arises from interactions between organic linkers with paddle-wheel units which are formed *in situ* rather than from a pre-formed dimetallic unit and the organic linker.[45] Thus, the success of its use as a secondary building unit[47] depends on reproducible assembly or retention of the paddle-wheel unit. We must make a clear distinction between assembling a MOF using organic linkers carrying terminal carboxylate groups which act as the donors in $\{M_2(\mu\text{-}O_2CR)_4\}$ or other metal carboxylate-based building blocks[47] and (as in this work) using metal acetate salts combined with organic linkers bearing donor atoms which bind in axial sites of $\{M_2(\mu\text{-}O_2CR)_4\}$ domains to generate coordination polymers. For the latter approach, pertinent examples of structural diversity come from reactions of $Cu(OAc)_2{\cdot}H_2O$ with bis(pyridine) ligands containing different backbones which lead to coordination polymers with various copper(II) acetate-containing nodes. With 1,4-bis(imidazole-1-yl)-methylene)benzene (bimb) in MeOH at reflux, $[Cu(O\text{-}OAc)_2(bimb)]_n$ is obtained in which square planar copper(II) centres are bridged by bimb; the metal nodes are, in this case, mononuclear (Scheme 4b).[48] Reaction of $Cu(OAc)_2{\cdot}H_2O$ with 4,4-bipyridine (4,4'-bpy) under hydrothermal

 

**Table 2** Parameters for $\pi_F\cdots\pi_F$ and $\pi_H\cdots\pi_H$ stacking interactions within the repeat unit (see Fig. 6)

| Biphenyl units containing atoms | $\pi_F\cdots\pi_F$ centroid···centroid/Å | $\pi_F\cdots\pi_F$ angle between ring planes/deg | $\pi_H\cdots\pi_H$ centroid···centroid/Å | $\pi_H\cdots\pi_H$ angle between ring planes/deg |
|---|---|---|---|---|
| F3/F8 | 3.66 | 5.6 | 3.69 | 6.7 |
| F8/F13 | 3.55 | 4.5 | 3.69 | 2.5 |
| F13/F18 | 3.52 | 7.1 | 3.75 | 9.9 |

| tpy units containing atoms | $\pi_H\cdots\pi_H$ centroid···centroid/Å | $\pi_H\cdots\pi_H$ angle between ring planes/deg |
|---|---|---|
| N1/N4 | 3.88 | 12.0 |
| N2/N5 | 3.73 | 1.8 |
| N3/N6 | 3.80 | 11.1 |
| N4/N7 | 3.80 | 8.1 |
| N5/N8 | 3.74 | 0.9 |
| N6/N9 | 3.75 | 3.9 |
| N7/N10 | 3.94 | 16.3 |
| N8/N11 | 3.79 | 1.6 |
| N9/N12 | 3.92 | 8.1 |

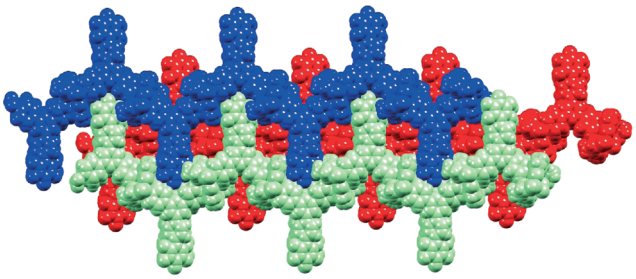

**Fig. 8** Packing of adjacent chains in $[Zn_5(OAc)_{10}(\mathbf{2})_4\cdot 11H_2O]_n$. The blue and green chains are in the same sheet (see text).

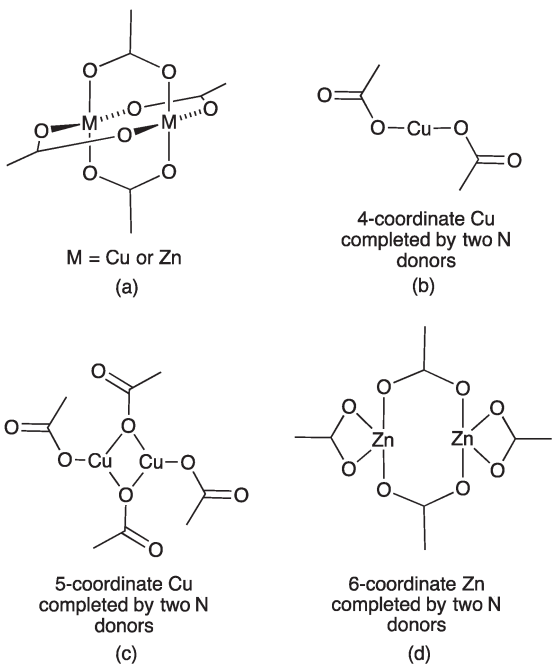


**Scheme 4** Examples of $\{M(OAc)_2\}_n$ motifs in coordination polymers of type $[M(OAc)_2(L)]_n$ and $[M_2(OAc)_4(L)]_n$ where L is a bis(pyridine) donor.

conditions yields a two-stranded coordination polymer directed by the $\{Cu_2(OAc)_4\}$ nodes shown in Scheme 4c. In contrast, under the same conditions, $Zn(OAc)_2\cdot 2H_2O$ reacts with 4,4'-bpy to give the two-stranded polymer containing the $\{Zn_2(OAc)_4\}$ units in Scheme 4d.[49] Crystallization of copper(II) acetate with 4,4'-dipyridylamine (dpa) under hydrothermal conditions results in $[Cu(O\text{-}OAc)_2(dpa)]_n$[50] (structurally similar to $[Cu(O\text{-}OAc)_2(bimb)]_n$), while room temperature crystallization of copper(II) acetate with 4-pyridylisonicotinamide (4-pina) yields a two-stranded polymer containing the $\{Cu_2(OAc)_4\}$ units in Scheme 4b.[50] In each of the above cases, a single analytically pure product is obtained in which the metal acetato assembly deviates from the more common paddle-wheel motif.

The results described in this and our earlier work[19,28–30,32] illustrate both predictable and unpredictable, and in some cases competitive, structural diversity among $\{M_x(OAc)_{2x}\}$ nodes ($x$ = 1, 2, 3, 5) leading to the formation of single-, double-, triple- or quadruple-stranded one-dimensional coordination polymers. Single-stranded coordination polymers containing $\{M_2(OAc)_4\}$ paddle-wheel nodes predominate and form in reactions of $Zn(OAc)_2\cdot 2H_2O$ with 4'-Ph-4,2':6',4''-tpy,[28] 4'-(4-$BrC_6H_4$)-4,2':6',4''-tpy,[29] 4'-(4-$MeSC_6H_4$)-4,2':6',4''-tpy,[29] 4'-$^t$Bu-4,2':6',4''-tpy[30] and **1**[19] and in reactions of $Cu(OAc)_2\cdot 2H_2O$ with **1**,[19] **2** and a 1 : 1 mixture of **1** and **2**. In these reactions, single products are isolated and elemental analyses for bulk samples are consistent with the stoichiometries confirmed crystallographically. In the case of $[Zn_2(\mu\text{-}OAc)_4(4'\text{-}Ph\text{-}4,2':6',4''\text{-}tpy)]_n$, we observe that crystallization over extended periods is accompanied by conversion of $[Zn_2(\mu\text{-}OAc)_4(4'\text{-}Ph\text{-}4,2':6',4''\text{-}tpy)]_n$ to $[Zn(O\text{-}OAc)_2(4'\text{-}Ph\text{-}4,2':6',4''\text{-}tpy)]_n$.[28]

The outcome of the reaction of $Zn(OAc)_2\cdot 2H_2O$ with **2** is unexpected and not readily explained. The anticipated single-stranded polymer $[Zn_2(\mu\text{-}OAc)_4(\mathbf{2})]_n$ is indeed formed, but the dominant crystalline product is the quadruple-stranded $[Zn_5(OAc)_{10}(\mathbf{2})_4\cdot 11H_2O]_n$. The remarkable feature of this polymer is the 5 : 4 ratio of zinc atoms : bridging ligands which leads to a deep (thick) chain constructed from interconnected, oblique $\{Zn_5(\mathbf{2})_4\}$ subchains (Fig. 7a). This assembly is a highly unusual 1D net, and Scheme 5 compares it to more commonly cited examples.[51,52] The net defined by all Zn atoms is shown in Scheme 5a, and the

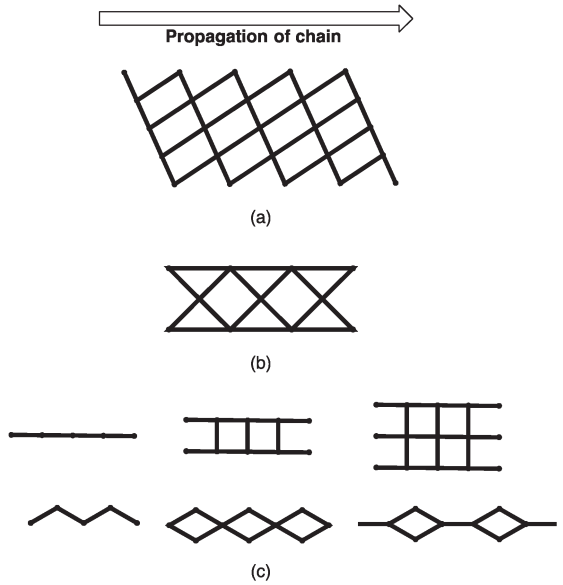


**Scheme 5** 1D nets: (a) and (b) in $[Zn_5(OAc)_{10}(\mathbf{2})_4{\cdot}11H_2O]_n$ (see text), and (c) more commonly cited examples.

Schläfli symbol with all Zn atoms as nodes (which thus includes two 2-connecting nodes, Zn1 and Zn5, which are normally reduced to links) is $(4)_2(4^3{\cdot}6^2{\cdot}8)_2(4^4{\cdot}6^2)$. If Zn1 and Zn5 are treated simply as links and omitted from the topological description (which is topologically more rigorous, but perhaps less chemically sensible), then the topology is reduced to that shown in Scheme 5b and the Schläfli symbol becomes $(3^2{\cdot}4.5^2{\cdot}6)_2(3^2{\cdot}4^2{\cdot}5^2)$. This net is in stark contrast to other multiple-stranded chains supported by 4'-X-4,2':6',4''-tpy bridging ligands. In both the double-stranded one-dimensional polymer $[Cd_2(OAc)_4(\mathbf{1})_2]_n$[19] and the triple-stranded $[Mn_3(OAc)_6(4'\text{-}(4\text{-}BrC_6H_4)\text{-}4,2':6',4''\text{-tpy})_3]_n$,[29] each Cd or Mn atom is connected to an N-donor of each of two 4,2':6',4''-tpy linkers leading to strand multiplicity that matches the nuclearity of the $\{M(OAc)_2\}_n$ node (Scheme 6a and b). Attempts to grow single crystals from the reaction of $Cd(OAc)_2{\cdot}2H_2O$ with **2** (see Experimental section) repeatedly produced poor quality crystals of $[Cd_2(\mu\text{-}OAc)_4(\mathbf{2})_2]_n$. Preliminary data confirmed the formation of a coordination polymer that is structurally analogous to $[Cd_2(OAc)_4(\mathbf{1})_2]_n$,[19] *i.e.* $\{Cd_2(\mu,\kappa^3\text{-}O,O':O'\text{-}OAc)_2(\kappa^2\text{-}O,O'\text{-}OAc)_2\}$ nodes (Scheme 6a) supporting double-stranded chains. In the unique $\{Zn(OAc)_2\}_5$ node in $[Zn_5(OAc)_{10}(\mathbf{2})_4{\cdot}11H_2O]_n$ (Scheme 6c), each of the terminal Zn atoms serendipitously binds only one N-donor.

Finally, whereas $[Zn(OAc)_2(4'\text{-X-}4,2':6',4''\text{-tpy})]_n$ polymers are chiral by virtue of a helical twist along the chain,[29,32] all of the polymers featuring $\{M(OAc)_2\}_n$ nodes ($n$ = 2, 3 or 5) are essentially flat ribbons with single-, double- or quadruple-stranded components. Irrespective of the internal assembly of each ribbon, the latter engage in similar inter-ribbon interactions ultimately giving π-stacked sheets.

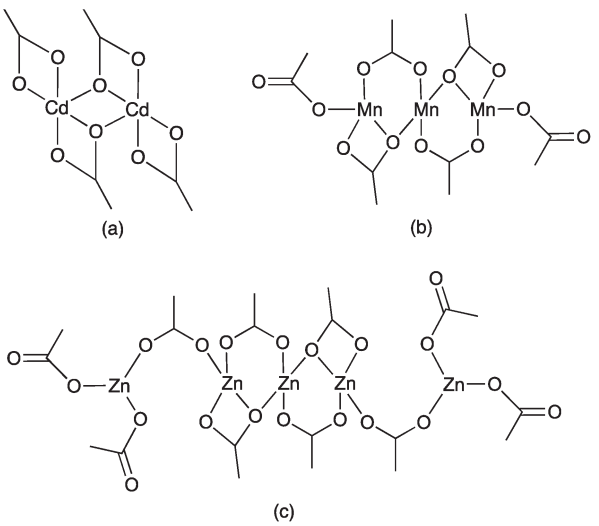


**Scheme 6** $\{M(OAc)_2\}_n$ motifs in coordination polymers containing 4'-X-4,2':6',4''-tpy and M = Cd, Mn and Zn.

## Conclusions

Coordination polymers formed from the pentafluoro derivative **2** and copper(II) or zinc(II) acetates have been prepared and structurally characterized, and their structures were compared with those produced with the all hydrogen analogue **1**. Reaction of **2** with $Cu(OAc)_2{\cdot}H_2O$ yields $[Cu_2(\mu\text{-}OAc)_4(\mathbf{2})]_n$ which is isostructural with $[Cu_2(\mu\text{-}OAc)_4(\mathbf{1})]_n$. When $Cu(OAc)_2{\cdot}H_2O$ reacts with a 1 : 1 mixture of **1** and **2**, $[Cu_2(\mu\text{-}OAc)_4(\mathbf{1})]_n$ and $[Cu_2(\mu\text{-}OAc)_4(\mathbf{2})]_n$ co-crystallize with **1** and **2** disordered over one ligand site, the whole assembly being isostructural with polymers $[Cu_2(\mu\text{-}OAc)_4(\mathbf{1})]_n$ and $[Cu_2(\mu\text{-}OAc)_4(\mathbf{2})]_n$. On going from $[Cu_2(\mu\text{-}OAc)_4(\mathbf{1})]_n$ to $[Cu_2(\mu\text{-}OAc)_4(\mathbf{2})]_n$, tpy···tpy π-stacking is retained, head-to-tail biphenyl···biphenyl $\pi_H{\cdots}\pi_H$ interactions are replaced by $\pi_H{\cdots}\pi_F$ contacts, and H···H contacts within sheets are replaced by H···F interactions. Significantly, the replacement of H by F substituents makes no difference to the overall solid-state structure.

With $Zn(OAc)_2{\cdot}2H_2O$, ligand **2** behaves unpredictably, forming $[Zn_5(OAc)_{10}(\mathbf{2})_4{\cdot}11H_2O]_n$ and $[Zn_2(\mu\text{-}OAc)_4(\mathbf{2})]_n$ as the dominant minor products, respectively. The latter is a one-dimensional polymer containing simple paddle-wheel nodes, while the former is constructed from $\{Zn_5(\mathbf{2})_4\}$ subchains interconnected by $\{Zn_5(OAc)_{10}\}$ units to generate infinite, quadruple-stranded polymer chains. These observations are surprising in the light of the predictable formation of $[Zn_2(\mu\text{-}OAc)_4(\mathbf{1})]_n$ as (apparently) the only product in the reaction of $Zn(OAc)_2{\cdot}H_2O$ and **1**.

In conclusion, our results based on reactions with copper(II) acetate suggest that perfluoroarene···arene and C–H···F interactions have little structural influence on 4,2':6',4''-terpyridine-based coordination polymers. In the spirit of 'one experiment too many', observations from products of reactions of ligands **1** and **2** with zinc(II) acetate highlight once again[53] the role of serendipity in directing the outcome of crystallization experiments.

## Acknowledgements

We thank the Swiss National Science Foundation, the European Research Council (Advanced Grant 267816 LiLo) and the University of Basel for financial support.

## Notes and references

1 See for example: D. O'Hagan, *Chem. Soc. Rev.*, 2008, **37**, 308; H. Amii and K. Uneyama, *Chem. Rev.*, 2009, **109**, 2119; E. Clot, O. Eisenstein, N. Jasim, S. A. Macgregor, J. E. McGrady and R. N. Perutz, *Acc. Chem. Res.*, 2011, **44**, 333; W. K. Hagmann, *J. Med. Chem.*, 2008, **51**, 4359; S. Purser, P. R. Moore, S. Swallow and V. Gouverneur, *Chem. Soc. Rev.*, 2008, **37**, 320.
2 S. K. Nayak, R. Sathishkumar and T. N. G. Row, *CrystEngComm*, 2010, **12**, 3112; and references therein.
3 N. Boden, P. P. Davis, C. H. Stam and G. A. Wesselink, *Mol. Phys.*, 1973, **25**, 81.
4 M. Nishio, *CrystEngComm*, 2004, **6**, 130.
5 M. Nishio, Y. Umezawa, K. Honda, S. Tsuboyama and H. Suezawa, Hiroko *CrystEngComm*, 2009, **11**, 1757.
6 S. Tsuzuki and A. Fujii, *Phys. Chem. Chem. Phys.*, 2008, **10**, 2584.
7 M. D. Prasanna and T. N. G. Row, *Cryst. Eng.*, 2000, **3**, 135.
8 J. S. W. Overell and G. S. Pawley, *Acta Crystallogr., Sect. B: Struct. Crystallogr. Cryst. Chem.*, 1982, **38**, 1966.
9 J. H. Williams, J. K. Cockcroft and A. N. Fitch, *Angew. Chem., Int. Ed. Engl.*, 1992, **31**, 1655.
10 See for example: G. W. Coates, A. R. Dunn, L. M. Henling, J. W. Ziller, E. B. Lobkovsky and R. H. Grubbs, *J. Am. Chem. Soc.*, 1998, **120**, 3641; J. C. Collings, K. P. Roscoe, E. G. Robins, A. S. Batsanov, L. M. Stimson, J. A. K. Howard, S. J. Clark and T. B. Marder, *New J. Chem.*, 2002, **26**, 1740; C. Knapp, E. Lork, R. Mews and A. V. Zibarev, *Eur. J. Inorg. Chem.*, 2004, 2446; J. C. Collings, J. M. Burke, P. S. Smith, A. S. Batsanov, J. A. K. Howard and T. B. Marder, *Org. Biomol. Chem.*, 2004, **2**, 3172; J. C. Collings, P. S. Smith, D. S. Yufit, A. S. Batsanov, J. A. K. Howard and T. B. Marder, *CrystEngComm*, 2004, **6**, 25; A. Hori and T. Arii, *CrystEngComm*, 2007, **9**, 215; I. Stoll, R. Brodbeck, B. Neumann, H.-G. Stammler and J. Mattay, *CrystEngComm*, 2009, **11**, 306; R. Xu, W. B. Schweizer and H. Frauenrath, *Chem.–Eur. J.*, 2009, **15**, 9105; B. Piotrkowska, M. Gdaniec, M. J. Milewska and T. Połoński, *CrystEngComm*, 2007, **9**, 686; L. M. Salonen, M. Ellermann and F. Diederich, *Angew. Chem., Int. Ed.*, 2011, **50**, 4808.
11 S. Bacchi, M. Benaglia, F. Cozzi, F. Demartin, G. Filippini and A. Gavezzotti, *Chem.–Eur. J.*, 2006, **12**, 3538.
12 K. Reichenbächer, H. I. Süss and J. Hulliger, *Chem. Soc. Rev.*, 2005, **34**, 22.
13 R. Berger, G. Resnati, P. Metrangolo, E. Weber and J. Hulliger, *Chem. Soc. Rev.*, 2011, **40**, 3496.
14 M. Stein, R. Berger, W. Seichter, J. Hulliger and E. Weber, *J. Fluorine Chem.*, 2012, **135**, 231.
15 See for example: M. Fujita, S. Nagao, M. Iida, K. Ogata and K. Ogura, *J. Am. Chem. Soc.*, 1993, **115**, 1574; K. Kasai, M. Aoyagi and M. Fujita, *J. Am. Chem. Soc.*, 2000, **122**, 2140.
16 T. M. Fasina, J. C. Collings, D. P. Lydon, D. Albesa-Jove, A. S. Batsanov, J. A. K. Howard, P. Nguyen, M. Bruce, A. J. Scott, W. Clegg, S. W. Watt, C. Viney and T. B. Marder, *J. Mater. Chem.*, 2004, **14**, 2395.
17 A. Hori, S. Takatani, T. K. Miyamoto and M. Hasegawa, *CrystEngComm*, 2009, **11**, 567.
18 K. Kasai, *Chem. Lett.*, 2006, **35**, 54.
19 E. C. Constable, C. E. Housecroft, M. Neuburger, J. Schönle, S. Vujovic and J. A. Zampese, *Polyhedron*, 2013, **60**, 20.
20 H. Irngartinger and T. Escher, *Tetrahedron*, 1999, **55**, 10753.
21 Bruker Analytical X-ray Systems, Inc., *APEX2, version 2 User Manual, M86-E01078*, Madison, WI, 2006.
22 G. M. Sheldrick, *Acta Crystallogr., Sect. A: Found. Crystallogr.*, 2008, **64**, 112.
23 I. J. Bruno, J. C. Cole, P. R. Edgington, M. K. Kessler, C. F. Macrae, P. McCabe, J. Pearson and R. Taylor, *Acta Crystallogr., Sect. B: Struct. Sci.*, 2002, **58**, 389.
24 C. F. Macrae, I. J. Bruno, J. A. Chisholm, P. R. Edgington, P. McCabe, E. Pidcock, L. Rodriguez-Monge, R. Taylor, J. van de Streek and P. A. Wood, *J. Appl. Crystallogr.*, 2008, **41**, 466.
25 J. Wang and G. S. Hanan, *Synlett*, 2005, 1251.
26 A. Wild, A. Winter, M. D. Hager, H. Görls and U. S. Schubert, *Macromol. Rapid Commun.*, 2012, **33**, 517.
27 F. H. Allen, *Acta Crystallogr., Sect. B: Struct. Sci.*, 2002, **58**, 380.
28 E. C. Constable, G. Zhang, C. E. Housecroft, M. Neuburger and J. A. Zampese, *CrystEngComm*, 2010, **12**, 2146.
29 E. C. Constable, G. Zhang, E. Coronado, C. E. Housecroft and M. Neuburger, *CrystEngComm*, 2010, **12**, 2139.
30 E. C. Constable, C. E. Housecroft, P. Kopecky, M. Neuburger, J. A. Zampese and G. Zhang, *CrystEngComm*, 2012, **14**, 446.
31 E. C. Constable, G. Zhang, C. E. Housecroft and J. A. Zampese, *Inorg. Chem. Commun.*, 2012, **15**, 113.
32 E. C. Constable, C. E. Housecroft, J. Schönle, S. Vujovic and J. A. Zampese, *Polyhedron*, 2013, **62**, 260.
33 J. D. Woodward, R. V. Backov, K. A. Abboud and D. R. Talham, *Polyhedron*, 2006, **25**, 2605.
34 B. Sun, Z. Wang and S. Gao, *Acta Sci. Nat. Univ. Pekin.*, 2001, **37**, 271, (refcodeMOKBIX01).
35 P. Phuengphai, S. Youngme, P. Kongsaeree, C. Pakawatchai, N. Chaichit, S. J. Teat, P. Gamez and J. Reedijk, *CrystEngComm*, 2009, **11**, 1723.
36 D. L. Reger, A. Debreczeni and M. D. Smith, *Inorg. Chim. Acta*, 2010, **364**, 10.
37 U. Kumar, J. Thomas and N. Thirupathi, *Inorg. Chem.*, 2010, **49**, 62.
38 P. Ren, M.-L. Liu, J. Zhang, W. Shi, P. Cheng, D.-Z. Liao and S.-P. Yan, *Dalton Trans.*, 2008, 4711.
39 H. Kwak, S. H. Lee, S. H. Kim, Y. M. Lee, B. K. Park, E. Y. Lee, Y. J. Lee, C. Kim, S.-J. Kim and Y. Kim, *Polyhedron*, 2008, **27**, 3484.
40 J.-H. Cai, Y.-H. Xu and S. W. Ng, *Acta Crystallogr., Sect. E: Struct. Rep. Online*, 2007, **63**, m2940.
41 H. Kwak, S. H. Lee, S. H. Kim, Y. M. Lee, B. K. Park, Y. J. Lee, J. Y. Jun, C. Kim, S.-J. Kim and Y. Kim, *Polyhedron*, 2009, **28**, 553.
42 Y.-Z. Zheng, M.-L. Tong and X.-M. Chen, *J. Mol. Struct.*, 2006, **796**, 9.

43 A. Karmakar, R. J. Sarma and J. B. Baruah, *Inorg. Chem. Commun.*, 2006, **9**, 1169.
44 C.-Y. Niu, X.-F. Zheng, Y. He, Z.-Q. Feng and C.-H. Kou, *CrystEngComm*, 2010, **12**, 2847.
45 M. Köberl, M. Cokoja, W. A. Herrmann and F. E. Kühn, *Dalton Trans.*, 2011, **40**, 6834.
46 S. I. Vagin, A. K. Ott and B. Rieger, *Chem. Ing. Tech.*, 2007, **79**, 767.
47 D. J. Tranchemontagne, J. L. Mendoza-Cortés, M. O'Keeffe and O. M. Yaghi, *Chem. Soc. Rev.*, 2009, **38**, 1257.
48 S. K. Chawla, M. Arora, K. Nättinen, K. Rissanen and J. V. Yakhmi, *Polyhedron*, 2004, **23**, 3007.
49 B. Conerney, P. Jensen, P. E. Kruger, B. Moubaraki and K. S. Murray, *CrystEngComm*, 2003, **5**, 454.
50 J. W. Uebler, B. S. Stone and R. L. LaDuca, *Z. Anorg. Allg. Chem.*, 2013, **639**, 1740.
51 S. R. Batten, S. M. Neville and D. R. Turner, *Coordination Polymers*, RSC Publishing, 2008, Chapter 2.
52 E. C. Constable, in *Supramolecular Chemistry: From Molecules to Nanomaterials*, ed. P. A. Gale and J. W. Steed, Wiley, 2012, vol. 6, p. 3073.
53 E. C. Constable, G. Zhang, C. E. Housecroft and J. A. Zampese, *CrystEngComm*, 2011, **13**, 6864.

 